ORGANIC LETTERS

2004
Vol. 6, No. 26
4929−4932

A Multifunctional High-Spin Biradical Pyrazolylbipyridine-bisnitronylnitroxide

Giorgio Zoppellaro, Volker Enkelmann, Ahmed Geies, and Martin Baumgarten*

Max Planck Institute for Polymer Research, Ackermannweg 10, D-55128, Mainz, Germany

baumgart@mpip-mainz.mpg.de

Received October 10, 2004

ABSTRACT

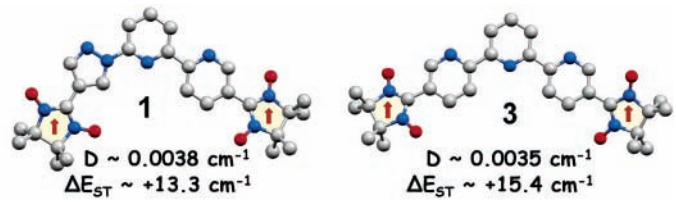

Synthesis and UV–vis, IR, and EPR spectroscopic characterizations, together with X-ray structural analysis, of functional nitronyl- and iminonitroxides attached to pyrazolylbipyridine are described. The exchange interactions between the nitronylnitroxides are found to be stronger than for the iminonitroxides. Although the substitution of a pyridine with the pyrazole ring leads to shorter distances and larger dipolar couplings, the exchange interaction is diminished. While compound 1 forms dimers in the solid state, the terpyridine 3 leads to supramolecular π-stacking.

Various approaches toward magnetic properties or molecular magnets with organic spin units have been dealt with experimentally and theoretically.[1] They can be classified into pure organic ones through synthesis of extended polyradicals or ordering of discrete radical molecules via π-stacking or hydrogen bonding and into the organic inorganic hybrid approach combining organic radicals with spin active metal ions or metal complexes. It has been demonstrated that linear alternating chains of nitronylnitroxides and M(hfac)$_2$ can be formed, even leading to ferro- or ferrimagnetic materials.[2] Therefore, high spin molecules with two or more nitronylnitroxides should not only help to extend the magnetic structures toward higher dimensions but also overcome the usual antiferromagnetic interaction between chains. We now report the synthesis of two such models, the organic biradicals 4″,5′-bis[3-oxide-1-oxyl-4,4,5,5-tetramethyl-imidazoli-din-2-yl]-6-(pyrazol-1″-yl)-2,2′-bipyridine **1** and the 4″,5′-bis[3-oxide-1-oxyl-4,4,5,5-tetramethyl-imidazolin-2-yl]-6-(pyrazol-1″-yl)-2,2′-bipyridine **2**. Because detailed studies of doubly disjoint[3] biradicals are scarce compared with nondisjoint systems,[4] we compare their structure and exchange coupling behavior to the previously reported terpyridines (**3** and **4**)[5] where now also the X-ray structure and the exchange couplings are elucidated (Scheme 1). We experimentally found that despite being doubly disjointed, their estimated through-bond exchange interaction (2J) is both ferromagnetic and unexpectedly large as compared with nondisjointed biradicals, like those based on disemiquinone and dinitroxide systems.[6] The assembly of diradicals **1** and **2** requires the synthesis of the nonsymmetric dicarbaldehyde **9**. This is achieved via a multistep synthetic approach involving Stille coupling of fragments **7** and **8** (Scheme 1)

(1) (a) *Magnetic Properties of Organic Materials*; Lahti, P. M., Ed.; Marcel Dekker: New York, 1999. (b) *Molecular Magnetism*; Kahn, O., Ed.; VCH: Cambridge, U.K., 1993. (c) *Magnetism: Molecules to Materials*; Miller, J. S., Drillon, M., Eds.; Wiley-VCH: Weinheim, 2001−2003; Vols. I−IV.

(2) (a) Caneschi, A.; Gatteschi, D.; Lalioti, N.; Sangregorio, C.; Sessoli, R. *J. Chem. Soc., Dalton Trans.* **2000**, *21*, 3907. (b) Minguet, M.; Luneau, D.; Lhotel, E.; Viller, V.; Paulsen, C.; Amabilino, D. B.; Veciana, J. *Angew. Chem., Int. Ed.* **2002**, *41*, 586.

(3) Matsumoto, T.; Ishida, T.; Koga, N.; Iwamura, H. *J. Am. Chem. Soc.* **1992**, *114*, 9952.

(4) Rajca, A. *Chem. Rev.* **1994**, *94*, 871.

(5) Zoppellaro, G.; Enkelmann, V.; Geies, A.; Baumgarten, M. *Polyhedron* **2003**, *22*, 2099.

(6) (a) Shultz, D. A.; Boal, K. A.; Lee, H.; Farmer, G. T. *J. Org. Chem.* **1999**, *64*, 4386. (b) Shultz, D. A. *Polyhedron* **2001**, *20*, 1627. (c) Shultz, D. A.; Fico, R. M.; Bodnar, S. H.; Kumar, R. K.; Vostrikova, K. E.; Kampf, J. W.; Boyle, P. D. *J. Am. Chem. Soc.* **2003**, *125*, 11761.

10.1021/ol0479040 CCC: $27.50
Published on Web 11/23/2004

Scheme 1

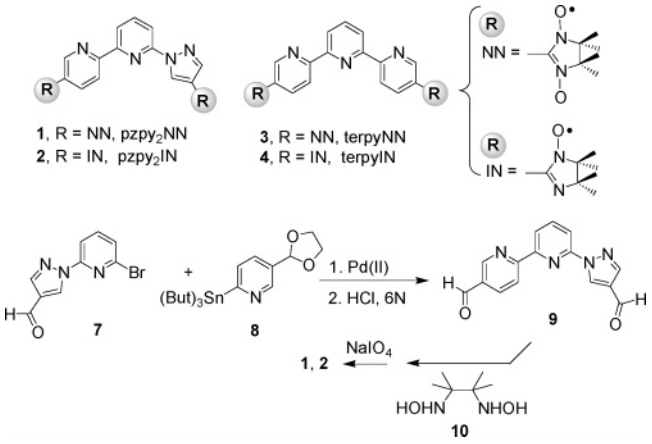

followed by acid hydrolysis of the acetal. Condensation of **9** with bis(hydroxylamino)-dimethylbutane **10** and then by periodate oxidation under phase transfer conditions affords **1** (9%) or **2** (18%) depending on the amount of oxidant used.

The blue nitronylnitroxide biradical **1** ($pzpy_2NN$) is stable as a solid and in toluene solutions. A typical broad band is observed in the visible spectrum (toluene, $\lambda_{max} = 610$ nm, $\epsilon = 1114$ M^{-1} cm^{-1}, $n \rightarrow \pi^*$ transition). Also the orange-red iminonitroxide biradical **2** ($pzpy_2IN$) shows similar stability, with the expected blue-shifted absorption (toluene, $\lambda_{max} = 467$ nm, $\epsilon = 1082$ M^{-1} cm^{-1}). Comparison with the earlier reported aminoxyl-oxide transitions in **3** (toluene, λ_{max} 605 nm, $\epsilon = 480$ M^{-1} cm^{-1})[5] and **4** (toluene, λ_{max} 459 nm, $\epsilon = 380$ M^{-1} cm^{-1})[5] show a hampered radical's optical absorption when the spin carriers are directly bound to the pyridine ring with respect to those directly connected to pyrazole moieties.[7] The IR of **1** features an intense ν_{N-O} stretching vibration at 1352 cm^{-1}, which is weaker and shifted in **2** ($\nu_{N-O} = 1371$ cm^{-1}). These are consistent both in frequency and intensity with those observed in **3**[5] and **4**.[5] Suitable crystals were grown in $CHCl_3$ for **1**[8] and in acetone for **3**.[9] Their structures are reported in Figure 1 together with structural parameters such as dihedral angles (Φ) and intramolecular radical distances. The two systems share nearly planar arrangements of the coupling core and rather small twisting angles between the imidazolyl and the pyridyl/pyrazolyl rings. Therefore, the geometrical prerequisite to enable excellent conjugation between the radical fragments through the coupler is ensured. The biradical **1** forms dimers in the solid state, where

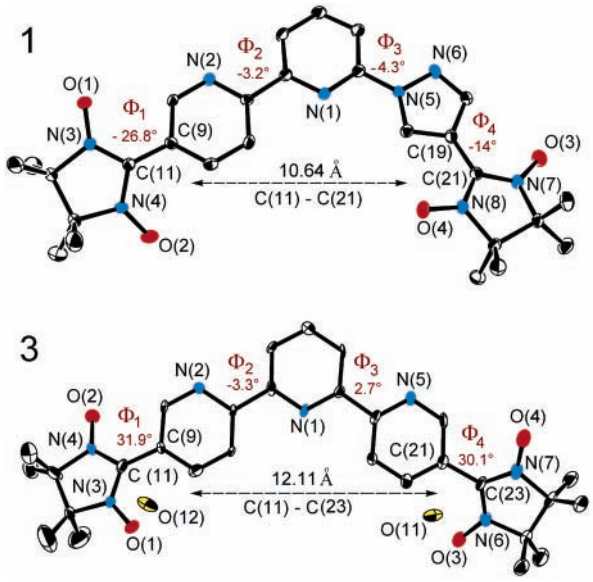

Figure 1. X-ray structures of **1** and **3** with ORTEP drawn at the 50% of the probability level. The hydrogen atoms are omitted for clarity.

inclusion of $CHCl_3$ prevents formation of extended π-networks. The biradical **3**, on the other hand, leads to a supramolecular stacking motif in solid state, with units 180° rotated on top to each at $d \sim 3.3$ Å.

Although such stacking arrangement should give rise to ferromagnetic chains, at 300 K the μ_{eff} value corresponds to 2.44 μ_B, consistent with the theoretical 2.45 μ_B for two uncorrelated spins, hence suggesting the near degeneracy of singlet and triplet states at high temperature. This value remains almost constant down to 70 K; then, it increases weakly, reaching a maximum at ~18 K (2.55 μ_B) followed by a sharp decrease at lower temperatures (Figure 2). The trend in μ_{eff} is analyzed in term of singlet−triplet equilibrium within the molecule, including an averaged intermolecular interaction, θ, adopting the mean-field approximation model.[10]

Such analyses provides a fairly large ferromagnetic through-bond interaction, with $2J/k_b = 29.4 \pm 5.6$ K, and an averaged antiferromagnetic through-space interaction $\theta = -2.6 \pm 0.2$ K (rms = 0.71). To obtain a better estimation of the ΔE_{S-T}, low-temperature EPR studies are then carried out on the dilute toluene solution of **3**. In this way, the

(7) Zoppellaro, G.; Geies, A.; Enkelmann, V.; Baumgarten, M. *Eur. J. Org. Chem.* **2004**, *11*, 2367.

(8) CCDC 229003. Formula for **1**: $C_{28}H_{33}N_8O_4Cl_3$, $M_w = 651.98$, triclinic, space group $P\bar{1}$ (no. 2), $a = 11.5796(4)$ Å, $b = 12.3160(5)$ Å, $c = 12.7410(5)$ Å, $\alpha = 69.9597(13)°$, $\beta = 65.7760(14)°$, $\gamma = 88.9354(12)°$, $V = 1540.85(11)$ Å^3, $\rho_c = 1.405$ g cm^{-3}, μ (Mo Kα/mm^{-1}) = 0.346, $Z = 2$, $T = 120$ K. Crystal color, shape, and size: blue, prism, 0.09 × 0.21 × 0.38 (mm). Dataset: 31 506 total, 8016 unique reflections ($4.0 < \upsilon < 29.0°$) of which 3793 were observed [$I_0 > 2.0\sigma(I_0)$], N_{ref} 3793, N_{par} 388, $S = 1.07$. The structure was solved by direct methods (SHELXS) and refined by a full-matrix least-squares procedure to R_1 value of 0.0512 ($wR_2 = 0.0571$, all data). The crystallographic data were collected on Nonius Kappa CCD (Mo Kα, $\mu = 0.71073$ Å) diffractometer equipped with a graphite monochromator. The full crystallographic details, excluding structure factors, were deposited with the Cambridge Crystallographic Data Centre.

(9) CCDC 234179. Formula for **3**: $C_{29}H_{37}N_7O_6$, $M_w = 579.66$, monoclinic, space group $P2_1/c$ (no. 14), $a = 6.5690$ Å, $b = 21.5610$ Å, $c = 20.6620$ Å, $\alpha = 90°$, $\beta = 90.8°$, $\gamma = 90°$, $V = 2926.16$ Å^3, $\rho_c = 1.316$ g × cm^{-3}, μ (Mo Kα/mm^{-1}) = 0.094, $Z = 4$, $T = 120$ K. Crystal color, shape, and size: blue, prism, 0.09 × 0.14 × 0.42 (mm). Dataset: 5870 total, 1924 unique reflections ($4.1 < \upsilon < 27.4°$) of which 1911 were observed [$I_0 > 2.0\sigma(I_0)$], N_{ref} 1911, N_{par} 379, $S = 1.07$. The structures were solved by direct methods (SHELXS) and refined by a full-matrix least-squares procedure to R_1 value of 0.0645 ($wR_2 = 0.0666$, all data). The crystallographic data were collected on Nonius Kappa CCD (Mo Kα, $\mu = 0.71073$ Å) diffractometer equipped with a graphite monochromator. The full crystallographic details, excluding structure factors, were deposited with the Cambridge Crystallographic Data Centre.

(10) Bino, A.; Johnston, D. C.; Goshorn, D. P.; Halbert, T. R.; Stiefel, E. I. *Science* **1988**, *241*, 1479.

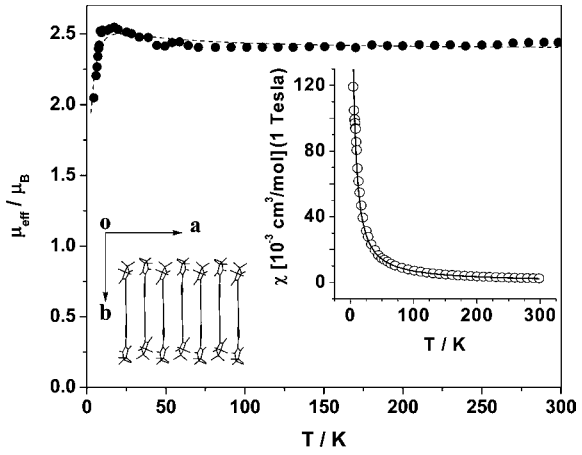

Figure 2. Plot of the observed magnetic susceptibility χ (○) and μ_{eff} (●, units in Bohr magneton μ_B) vs temperature (T, in K) for the crystalline sample of biradical **3**. The inset shows a view down the crystallographic c-axis of a section for the π-stacking of **3**. The best fit curves for μ_{eff} and χ are shown as dashed and plain lines with parameters given in the text.

intermolecular contributions are made negligible (vide infra). The liquid solution EPR spectra (toluene) exhibits 9 lines for **1** (g_{iso} = 2.0066(1)) and 13 lines for **2** (g_{iso} = 2.0061-(1)), confirming the strong exchange coupling ($J \gg a_N$) between the radical fragments. A lower limit of $|J/a_N| \geq 45$ (i.e., $|2J/k_b| \geq 0.06$ cm^{-1}) is extracted upon simulations of their entire EPR envelopes, without, however, gaining knowledge of the sign of J. In frozen solution, the typical zero-field-splitting (zfs) components of $|D/hc| = 3.8 \times 10^{-3}$ cm^{-1} for **1** and $|D/hc| \sim 3.9 \times 10^{-3}$ cm^{-1} for **2** were detected, corresponding to $r \sim 8.8$ and 8.7 Å from a point dipole approach,[11] together with the forbidden $\Delta m_s = 2$ transitions at half field ($g_{av} \sim 4.01$).

At rt and at 120 K, the ratio of double-integrated intensity of the $\Delta m_s = 1$ transitions for **1**−**4** were only 2:1 compared with related monoradicals. Such information already provides the range of energies in which the singlet−triplet gaps are located (0.06 cm^{-1} ≤ $|\Delta E_{S-T}|$ ≤ 83 cm^{-1}). The intensities of the forbidden $\Delta m_s = 2$ signals increased in both **1** and **2** almost linearly upon lowering the temperature down to 4 K (Curie-like). The product DI × T vs T, on the other hand, increased upon lowering the temperature (Figure 3A) for **1**, showing its full triplet occupation. Fitting the DI × T data according to the Bleaney−Bowers model[12] for two interacting $S = 1/2$ systems gave $2J = \Delta E_{S-T} = 13.3 \pm 4.9$ cm^{-1} for **1**. For **2**, the singlet−triplet gap, however, is much smaller and falls in the range of 0.06 cm^{-1} ≤ ΔE_{S-T} ≤ 0.7 cm^{-1} (Figure 3B) with the lower limit being consistent with the rt simulation of its EPR envelope. These findings confirm the greater proclivity of nitronylnitroxides to adopt high-spin ground states compared to iminonitroxides. For the terpyridine biradicals **3** and **4**, careful control of the low-

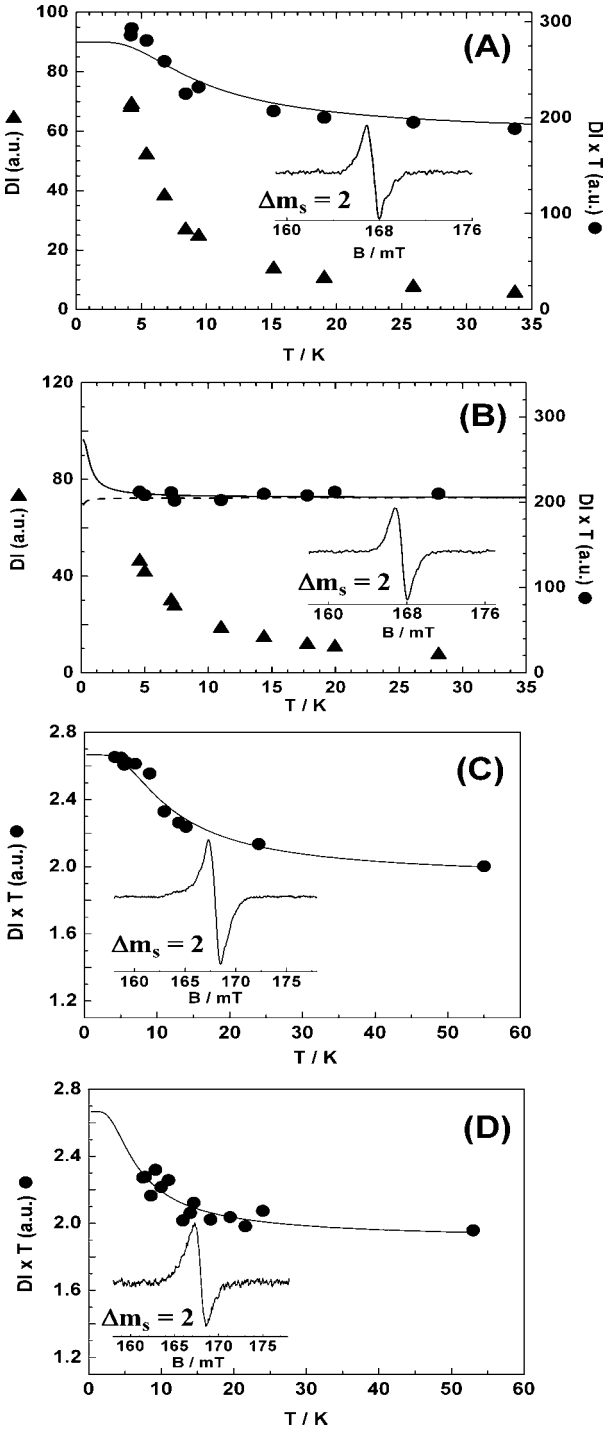

Figure 3. Evolution of the double-integrated signal intensities (DI, ▲) and the product DI × T (●) vs T of the $\Delta m_s = 2$ signal for **1** (**A**), **2** (**B**), **3** (**C**), and **4** (**D**) in the low-temperature range. The solid lines represent the theoretical fitting according to the Bleaney−Bower model, and the insets show the observed $\Delta m_s = 2$ transition at the lowest temperatures (T = 4 K for (**A**), (**B**), and (**C**), T = 7 K for (**D**)). The dashed line in (**B**) shows the fitting assuming the singlet ground state ($S = 0$) and the solid line shows the fitting for the triplet ground state ($S = 1$).

temperature data of the $\Delta m_s = 2$ transitions followed by the DI × T vs T fitting yielded a more accurate ΔE_{S-T} = 15.4

(11) *Electron Paramagnetic Resonance*; Weil, J. A.; Bolton, J. R.; Wertz, J. E., Eds.; VCH−Wiley Interscience: New York, 1994; p 174.
(12) Bleaney, B.; Bowers, K. *Proc. R. Soc. London* **1952**, A214, 451.

$\pm$ 2.0 cm^{-1} for **3** (Figure 3C) and the smaller $\Delta E_{S-T} = 8.7 \pm 1.0$ cm^{-1} for **4** (Figure 3D). Thus, although the shorter distance in pyrazole-containing biradicals **1** and **2** leads to enhanced dipolar couplings (*zfs*) compared to **3** and **4**, the exchange interaction is lowered. This is due to the occurrence of two different pathways for the spin-polarization in **1** and **2**, arising from the presence of a five-membered ring (pyrazole).

In conclusion, we have described new biradicals and compared their structure and exchange interaction, which is sizable and ferromagnetic. In contrast with previous reports in similar pyridine-based nitronylnitroxide biradical systems,[13] where no significant intramolecular interactions are found, the present work shows an efficient propagation of the spin polarization through bond even when a second or a third pyridine ring is introduced as a spacer. Their use in extended networks through their radical units and/or size recognition of their tridentate nitrogen binding cage is presently underway. Such functionalized cores, even without radical units, may further be considered as ligands for promising spin-crossover compounds.[14]

Acknowledgment. Support by the DFG and the Max Planck Society is gratefully acknowledged. The authors thank Prof. W. Haase and Dr. K. Falk (TU Darmstadt) for the magnetic susceptibility measurements.

Supporting Information Available: Detailed synthetic procedures toward biradicals **1** and **2**, ^{1}H, ^{13}C NMR, UV−vis, and IR data, EPR in solution for **1** and **2** (with simulations), in the frozen state and power saturation behaviors for all the radical systems, and X-ray structures of **1**, **3**, and a monoradical (which was used for spin quantization) in CIF format. This material is available free of charge via the Internet at http://pubs.acs.org.

OL0479040

(13) (a) Ziessel, R.; Ulrich, G.; Lawson, R. C.; Echegoyen, L. *J. Mater. Chem.* **1999**, *9*, 1435. (b) Romero, F. M.; Ziessel, R. *Tetrahedron Lett.* **1999**, *40*, 1895. (c) Ziessel, R. *Mol. Cryst. Liq. Cryst.* **1995**, *273*, 101. (d) Stroh, C.; Ziessel, R. *Tetrahedron Lett.* **1999**, *40*, 4543.

(14) Money, V. A.; Evans, I. R.; Halcrow, M. A.; Goeta, A. E.; Howard, J. A. K. *Chem. Commun.* **2003**, 158.